JOURNAL OF MATERIALS SCIENCE 11 (1976) 1066–1076

Precipitation of equilibrium phases in vapour-quenched Al-Ni, Al-Cu and Al-Fe alloys

B. CANTOR, R. W. CAHN
Materials Science Laboratory, School of Applied Sciences, University of Sussex, Falmer, Brighton, Sussex, UK

In situ annealing experiments in the transmission electron microscope have been used to investigate the thermal stability and precipitation behaviour of non-equilibrium phases in vapour-quenched Al–Ni, Al–Cu and Al–Fe alloys prepared by co-sputtering. The non-equilibrium phases exhibit surprisingly high thermal stability and the general nature of precipitation is different from that in liquid-quenched or conventional alloys. These phenomena are caused by the very small as-quenched grain size.

1. Introduction

In a recent paper [1], we describe an investigation into the non-equilibrium phases formed in vapour-quenched Al–Ni, Al–Cu and Al–Fe alloys prepared by co-sputtering. The results may be summarized briefly as follows:

(1) In co-sputtered films ~ 1000 to 2000 Å thick the alloys are polycrystalline with an equiaxed grain size of ~ 50 Å.

(2) At compositions of 0 to 20.9 at.% Ni, 0 to 28.5 at.% Cu and 0 to 12.9 at.% Fe, the vapour-quenched alloys form highly supersaturated solid solutions of f c c (Al).

(3) In alloys with more than 12.9 at.% Fe the vapour-quenched phases are identical to those formed under equilibrium conditions.

(4) Between 42.5 to 78.8 at.% Ni and 47.6 to 60.0 at.% Cu, vapour-quenched Al–Ni and Al–Cu have a non-equilibrium disordered b c c structure.

(5) At compositions between the f c c solubility limit and the onset of the disordered b c c phase, vapour-quenched Al–Ni and Al–Cu have an anomalous structure which could be either a strongly textured single f c c phase, or an f c c/amorphous phase mixture.

The objective of the present work was to investigate the formation of equilibrium phases from vapour-quenched Al–Ni, Al–Cu and Al–Fe alloys, by means of *in situ* heating experiments in a transmission electron microscope.

2. Experimental technique

Alloys of a variety of compositions were deposited by co-sputtering from 99.999% pure sectored sheets of the constituent elements, in an r.f. getter-sputtering unit [2, 3] (Fig. 1). Details of the sputtering apparatus and operating procedure have been described previously [1]. The sputtering gas was 99.9% pure argon which was further purified by a getter in the sputtering chamber. During deposition, the gas pressure was ~ 10^{-2} Torr, the r.f. power was 0.5 to 1.0 kW, and the axial magnetic field was 20 to 30 Oe. Alloys were deposited at ~ 2 Å sec^{-1} onto 1 mm thick cleaved slices of NaCl single crystal, bonded onto 1.5 mm thick copper sheet which was cooled directly with liquid nitrogen and rotated at ~ 60 rpm during deposition. The alloy films prepared in this way were typically 2000 to 3000 Å thick.

Deposited films were removed from the substrate by dissolving the NaCl in water, and were examined in an AEI EM6G transmission electron microscope. Specimens were heat-treated directly in the microscope using a specimen stage which was heated by passing an electric current through a stainless steel support grid. This method produced some thermal gradients, particularly through the specimen thickness. Temperatures were measured by calibration against the melting points of several pure metals, but this was not very accurate because of variations in specimen thermal

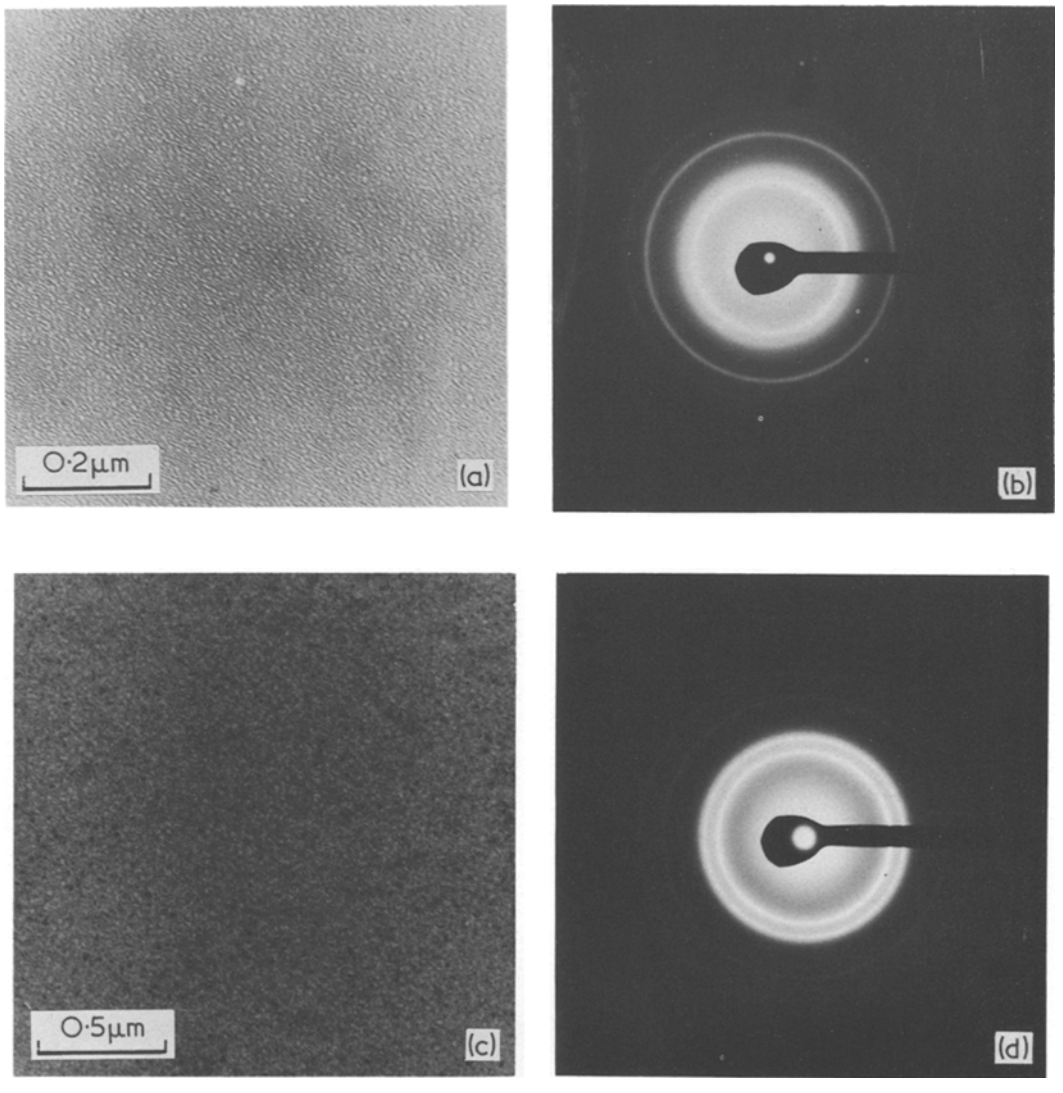

Figure 1 Grain growth in vapour-quenched Al–11.3 at.% Ni: (a) and (b) as-deposited showing supersaturated f c c grains ~ 50 Å in size; (c) and (d) after 3 min at 300° C showing supersaturated f c c grains ~ 200 Å in size.

mass, the presence of thermal gradients, and the effects of electron beam heating. Each film was step-annealed for 10 min at each temperature, the temperature increasing successively by increments of 50 K until precipitation of equilibrium phases was observed. Film compositions were measured on specially prepared 1 to 2 μm thick films by X-ray microanalysis using an ORTEC analyser attached to a Cambridge Stereoscan 2 A scanning electron microscope, at an accelerating voltage of 5 kV. Details of the analysis procedure have been described previously [1].

3. Results

Table I shows the compositions of alloys investigated by *in situ* heating in the electron microscope. For each composition, the table lists the vapour-quenched and equilibrium phases, the melting point, and the lowest temperature for which precipitation was initiated with 10 min.

Precipitation from a supersaturated f c c (Al) solid solution was always preceded by a period of grain growth in which the as-quenched grain size of ~ 50 Å increased to ~ 200 Å. Figure 1 shows an example of grain growth in an alloy of

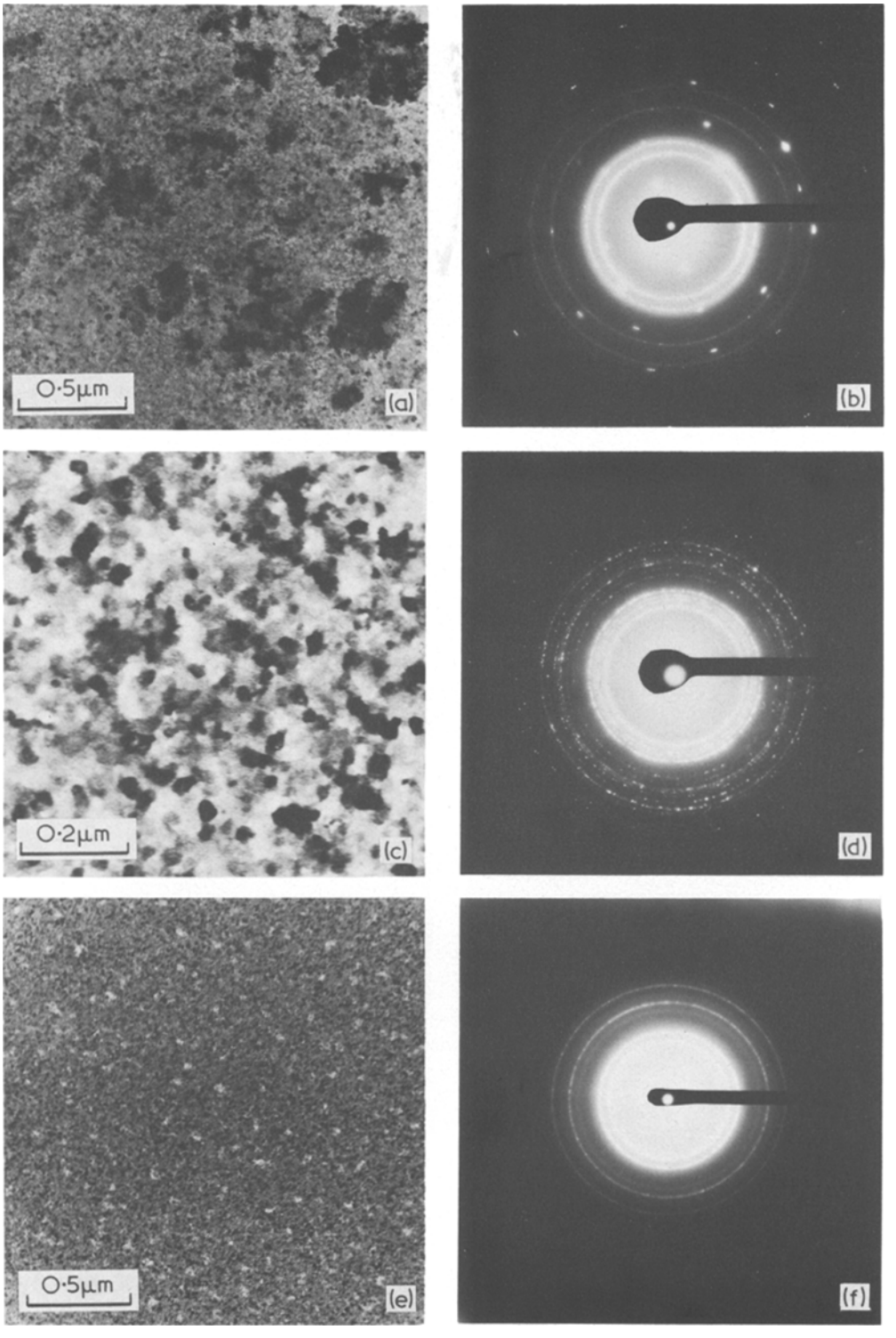

Figure 2 Precipitation of equilibrium phases from supersaturated f c c alloys: (a) and (b) Al–11.3 at.% Ni after 10 min at 300° C showing 2000 to 3000 Å particles of $NiAl_3$ in an f c c (Al) matrix; (c) and (d) Al–20.5 at.% Cu after 2 min at 350° C showing 300 to 600 Å particles of $CuAl_2$ in an f c c (Al) matrix; (e) and (f) Al–7.7 at.% Fe after 3 min at 500° C showing 200 to 300 Å particles of $FeAl_3$ in an f c c (Al) matrix.

TABLE I Precipitation data for vapour-quenched Al–Ni, Al–Cu and Al–Fe

Alloy	Composition (at.% Ni, Cu or Fe)	Vapour-quenched phases	Equilibirum phases	Precipitation temperature T_p(° C)
Al–Ni	11.3	f c c (Al)	f c c (Al) + orthorhombic ($NiAl_3$)	300
	20.9	f c c (Al)	f c c (Al) + orthorhombic ($NiAl_3$)	400
	25.0	anomalous f c c	orthorhombic ($NiAl_3$)	300
	29.2	anomalous f c c	orthorhombic ($NiAl_3$) + ordered b c c (Ni_2Al_3)	450
	39.5	anomalous f c c	ordered b c c (Ni_2Al_3)	300
	42.5	disordered b c c	ordered b c c (Ni_2Al_3) + ordered b c c (NiAl)	300
	55.2	disordered b c c	ordered b c c (NiAl)	350
	72.4	disordered b c c	ordered b c c (NiAl) + ordered f c c (Ni_3Al)	300
	78.8	disordered b c c	ordered f c c (Ni_3Al) + f c c (Ni)	800
	83.8	f c c (Ni)	ordered f c c (Ni_3Al) + f c c (Ni)	500
Al–Cu	20.5	f c c (Al)	f c c (Al) + tetragonal ($CuAl_2$)	350
Al–Fe	7.7	f c c (Al)	f c c (Al) + monoclinic ($FeAl_3$)	500
	12.9	f c c (Al)	f c c (Al) + monoclinic ($FeAl_3$)	550

Al–11.3 at.% Ni. Electron diffraction patterns showed that the alloys retained their supersaturated f c c structure during this process. Variations in intensity of f c c diffraction rings indicated that deposition textures were removed during grain growth. The supersaturated Al–Fe alloys were more resistant to grain growth than were Al–Ni or Al–Cu alloys. In both Al–Ni and Al–Fe, the temperature required to initiate grain growth increased with increasing supersaturation. Further heat treatment at the same temperature led to precipitation of $NiAl_3$, $CuAl_2$ or $FeAl_3$ particles of ~ 500 Å diameter, followed by continued particle growth to sizes of 2000 to 3000 Å (Fig. 2).

The precipitation behaviour of vapour-quenched Al–25 at.% Ni was markedly different from that of the other alloys investigated. In all other alloys, precipitation was on a fine scale (initially ~ 150 to 300 Å) with copius nucleation and slow growth. In Al–25 at.% Ni, precipitation was initiated by sparse nucleation, followed by very rapid growth of large crystals of $NiAl_3$ (Fig. 3). Table II shows relative growth rates for a number of precipitation processes in vapour-quenched aluminium alloys, measured from a series of micrographs similar to Fig. 3. In each case, the growth rate was measured at the lowest temperature at which precipitation was observed within 10 min, ensuring an approximate comparability of the data in Table II. Each growing particle of $NiAl_3$ was approximately disc-shaped and reached a final diameter of ~ 30 μm and a thickness equal to the foil thickness of ~ 2000 Å. Each particle consisted of a few single crystals, each containing a large number of low-angle sub-boundaries; the grain boundaries and sub-boundaries radiated from the central nucleating point. Figure 4 shows the boundary between an $NiAl_3$ particle and the untransformed matrix, with grooves at a grain boundary and several sub-boundaries.

TABLE II Approximate growth rates during precipitation

Alloy	Precipitate	Approximate growth rate (Å sec^{-1})
Al–11.3 at.% Ni	grain growth	1
Al–11.3 at.% Ni	$NiAl_3$	10
Al–7.7 at.% Fe	$FeAl_3$	2.5
Al–20.5 at.% Cu	$CuAl_2$	4
Al–25.0 at.% Ni	$NiAl_3$	150
Al–55.2 at.% Ni	NiAl	0.1
Al–72.4 at.% Ni	Ni_3Al	5
Al–29.2 at.% Ni	$NiAl_3$	33
Al–78.8 at.% Ni	Ni_3Al	80

For all Al–Ni alloys in the range 29.2 to 72.4 at.% Ni, the first stage of precipitation was the formation of 150 to 200 Å single phase grains with an ordered b c c structure similar to the equilibrium NiAl phase (isotypic with CsCl). For Al–55.2 at.% Ni, this was the equilibrium structure and no further change was observed (Fig. 5). Alloys of Al–72.4 at.% Ni had to be heated to a higher temperature to induce the further precipitation of internally twinned Ni_3Al particles, 2000 to 3000 Å in size (Fig. 6a and b). In alloys of 29.2, 39.5 and 42.5 at.% Ni, equilibrium phases were precipitated from the ordered b c c phase without a further increase in temperature (Fig. 6c

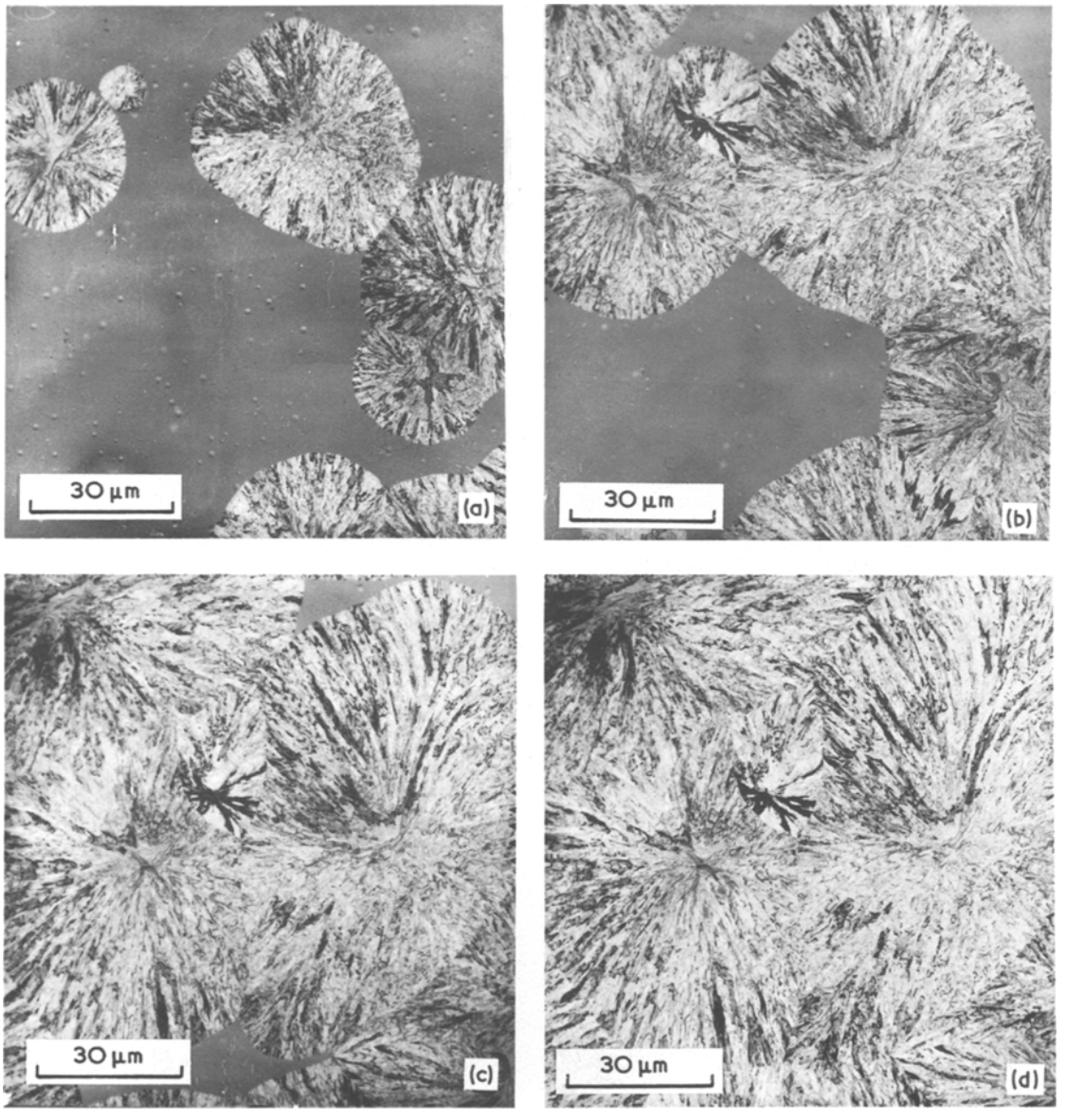

Figure 3 Precipitation of $NiAl_3$ from vapour-quenched Al–25 at.% Ni: (a) after 6 min at 300° C; (b) same area after 14 min at 300° C; (c) same area after 19 min at 300° C; (d) same area after 25.5 min at 300° C.

to f). In each case, this involved a re-ordering process to convert some or all of the NiAl-type ordered b c c phase into Ni_2Al_3-type ordered b c c. In Al–29.2 at.% Ni, this re-ordering process was concurrent with the precipitation of 2 to 3 μm particles of $NiAl_3$.

The equilibrium structure of alloys containing 78.8 and 83.8 at.% Ni was a phase mixture of Ni_3Al and f c c (Ni). In Al–83.8 at.% Ni, Ni_3Al particles were precipitated directly from the as-quenched supersaturated f c c (Ni). In Al–78.8 at.% Ni the as-quenched structure was disordered b c c and precipitation took place in two stages; an initial transformation of disordered b c c into supersaturated f c c, followed immediately by rapid precipitation of Ni_3Al particles (Fig. 7).

4. Discussion

The overall precipitation sequence in vapour-quenched supersaturated f c c aluminium alloys

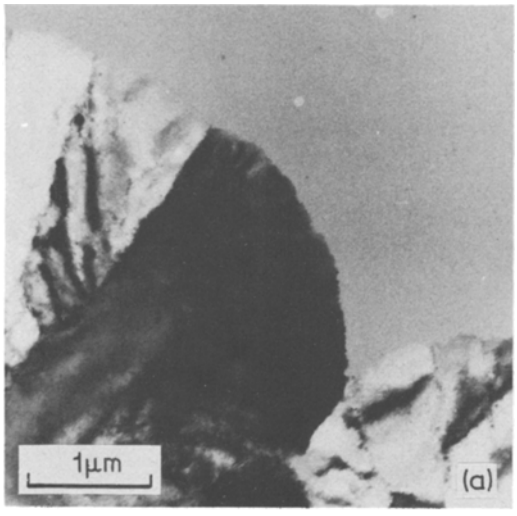

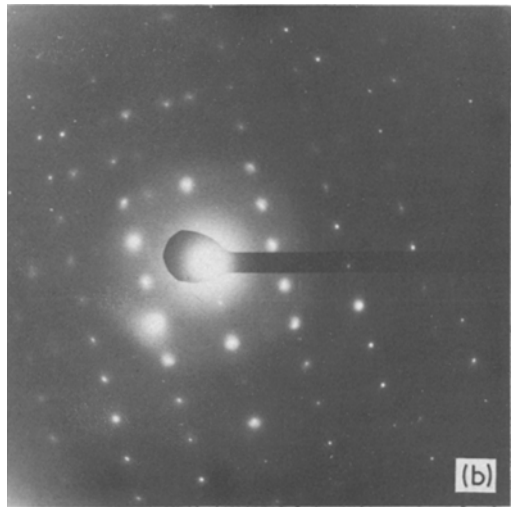

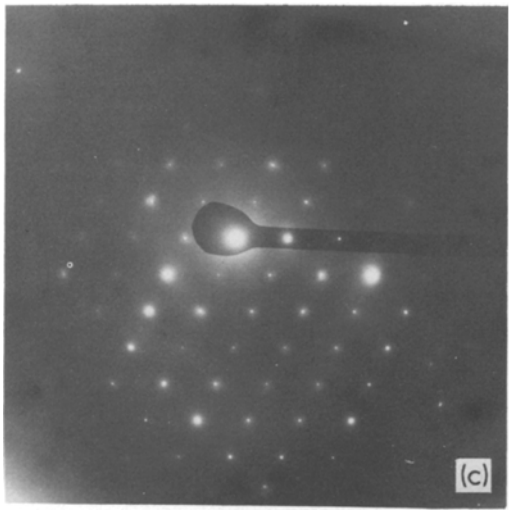

Figure 4 (a) Boundary of growing $NiAl_3$ particle showing a large groove at a grain boundary and smaller grooves at several sub-boundaries. (b) and (c) Diffraction patterns from the two grains in (a).

is very different from that observed in supersaturated aluminium alloys prepared by either liquid-quenching [4–10] or conventional solid-state quenching [11]. Firstly, the vapour-quenched alloys are more resistant to annealing. Secondly, the precipitation sequence involves an initial period of grain growth. Thirdly, there is apparently no formation of GP zones or intermediate phases.

Table I indicates that vapour-quenched supersaturated aluminium alloys are stable up to 300 to 400° C for Al–Ni and Al–Cu, and 500 to 550° C for Al–Fe, whereas conventional alloys decompose at temperatures below 200° C [11]. To some extent, this discrepancy may be caused by relatively inaccurate temperature measurements in the present experiments (see section 2). However, enhanced thermal stability has been observed in highly supersaturated liquid-quenched Al–Ni [4, 5, 12], Al–Cu [6, 7, 13] and Al–Fe alloys [8, 9, 12, 14], and may be caused by low vacancy concentrations. Thomas and Willens [15] have claimed that liquid-quenched aluminium foils contain low vacancy concentrations because quenched-in vacancies can diffuse to the foil surfaces, although this conclusion has been disputed [16]. However, in vapour-quenched foils, the grain size of ~ 50 Å is considerably less than the width of precipitate-free zones formed during ageing of conventional aluminium alloys [11]. Therefore, the grain boundaries in vapour-quenched alloys can act as sites for all excess quenched-in vacancies, producing low solute mobility and high resistance to thermal treatment.

Grain growth and the absence of GP zones and intermediate phases can also be explained as consequences of the small grain size in the vapour-quenched alloys. Because of the low vacancy concentration and correspondingly low solute mobility, the alloys are stable up to temperatures at which grain boundaries begin to migrate. For short annealing times, the large surface area and high curvature of grain boundaries promote rapid grain growth. For longer annealing times, precipitates can form by relatively long-range solute diffusion. In this latter stage, conventional solute diffusion by solute-vacancy interactions may be

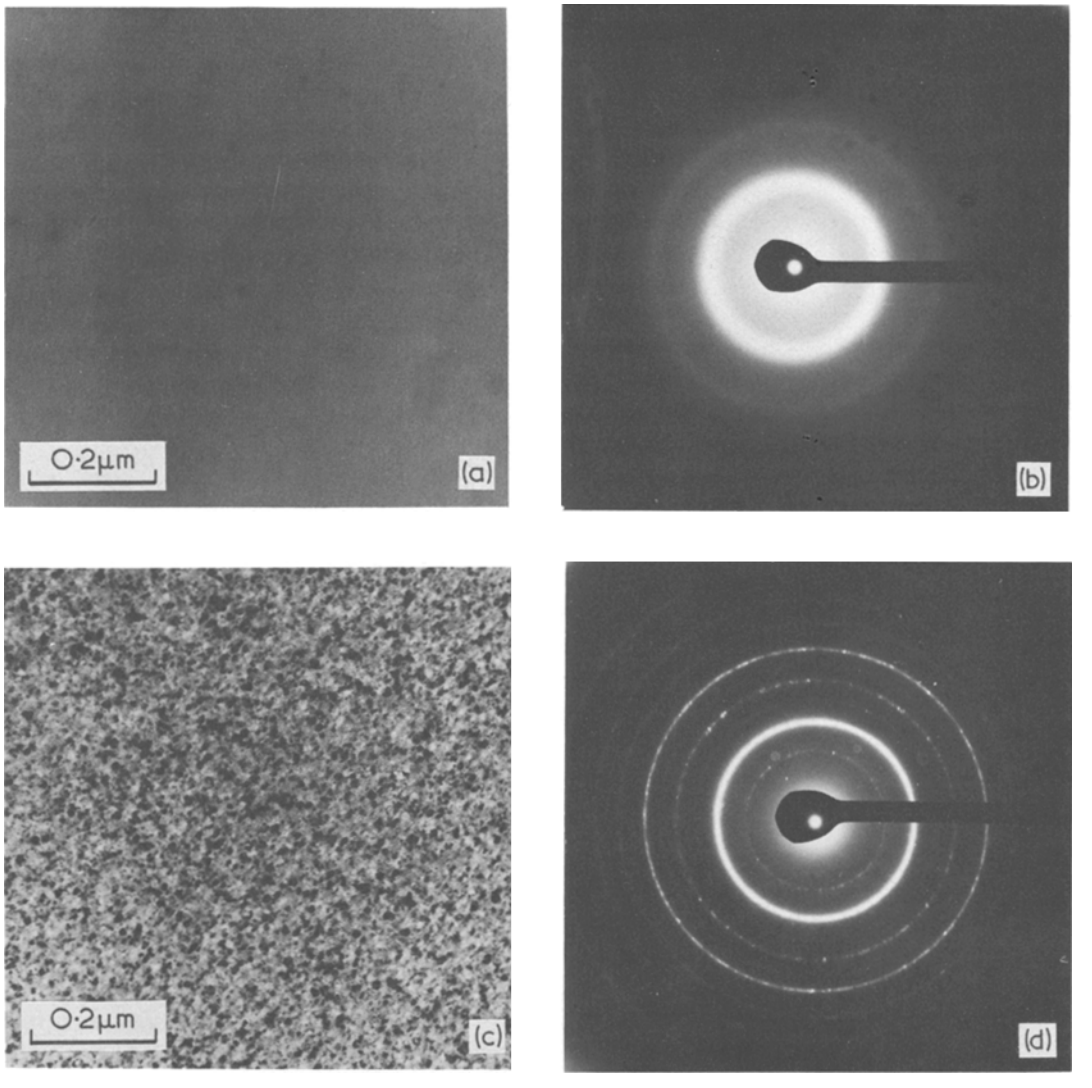

Figure 5 Precipitation of NiAl in Al–55.2 at.% Ni: (a) and (b) as-deposited showing disordered b c c grains ~ 50 Å in size; (c) and (d) after 14 min at 350° C showing NiAl grains ~ 150 Å in size.

enhanced by the action of moving grain boundaries in sweeping-up solute atoms. In conventional alloys, GP zones and intermediate phases form because of their favourable kinetics. In vapour-quenched alloys, the extensive grain boundaries, especially when in motion, provide sufficient heterogeneous nucleation sites to counteract the strain energy barrier which normally inhibits precipitation of incoherent equilibrium phases. It might be argued that if GP zones did form, their presence would not be detected on diffuse electron diffraction ring patterns. However, the concept of GP zones is not very meaningful in an alloy with a grain size equal to or less than the size of the GP zones.

In equilibrium Al–Ni alloys there are two ordered b c c phases [17]. The NiAl phase exists over the composition range 45.0 at.% Ni to 69.5 at.% Ni [17]. It is isotypic with CsCl, and at the equiatomic composition consists of two interpenetrating simple cubic sub-lattices of nickel and aluminium such that nickel atoms are at cube centres and aluminium atoms at cube corners [18]. In nickel-rich alloys, nickel atoms replace aluminium atoms substitutionally; in aluminium-rich alloys, vacancies are formed on the nickel sub-lattice [18]. At the equilibrium phase boundary, ~ 25% of the nickel sites are vacant. The Ni_2Al_3 phase exists over the composition range 36.3 at.% Ni to 40.8 at.% Ni [17]. Its structure is

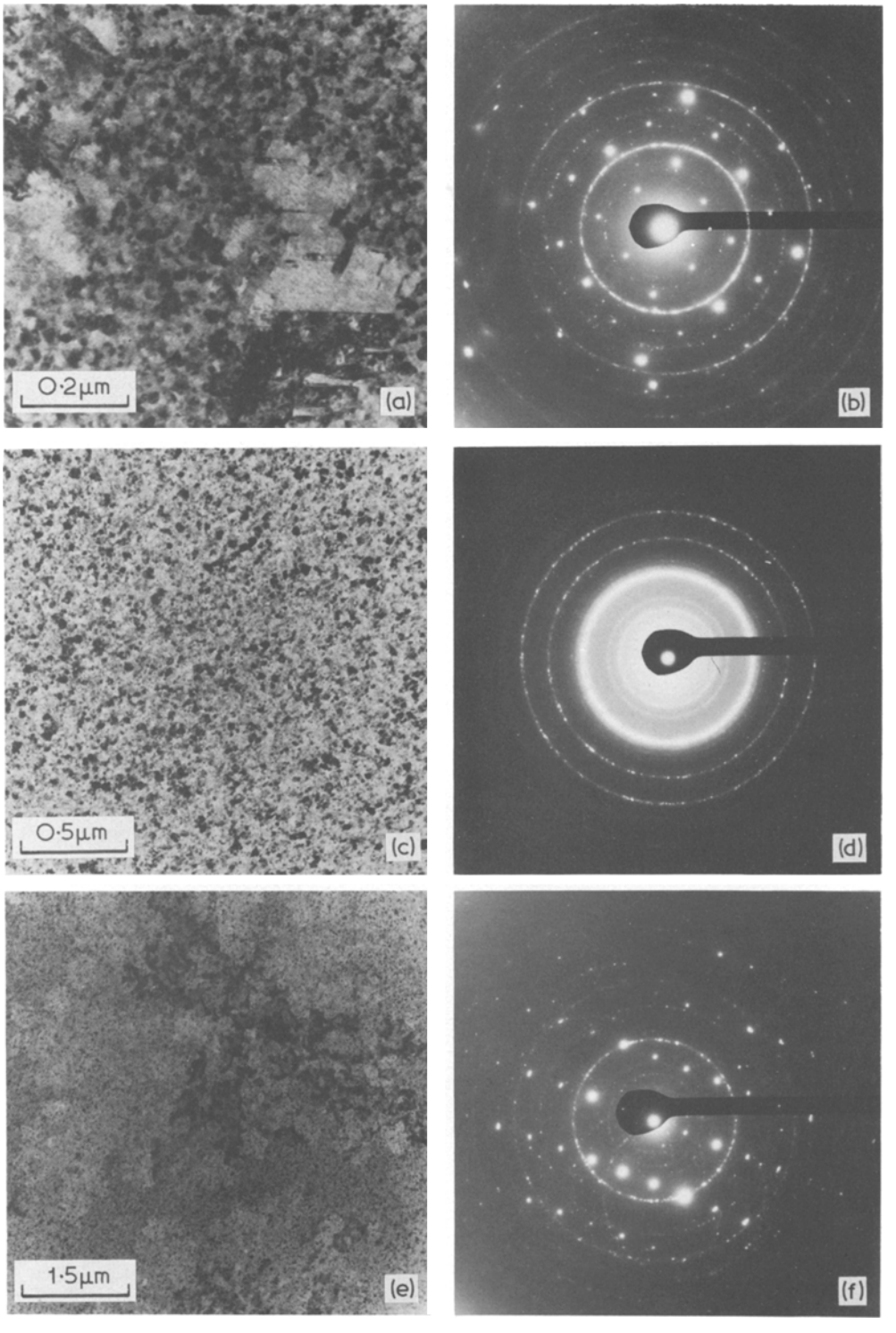

Figure 6 Precipitation of equilibrium phases from metastable ordered b c c (NiAl): (a) and (b) Al–72.4 at.% Ni after 10 min at 500° C showing ~ 3000 Å twinned particles of Ni_3Al in an NiAl matrix; (c) and (d) Al–39.5 at.% Ni after 7 min at 300° C showing Ni_2Al_3 grains ~ 300 Å in size; (e) and (f) Al–29.2 at.% Ni after 15 min at 450° C showing ~ 3 μm particles of $NiAl_3$ in an Ni_2Al_3 matrix.

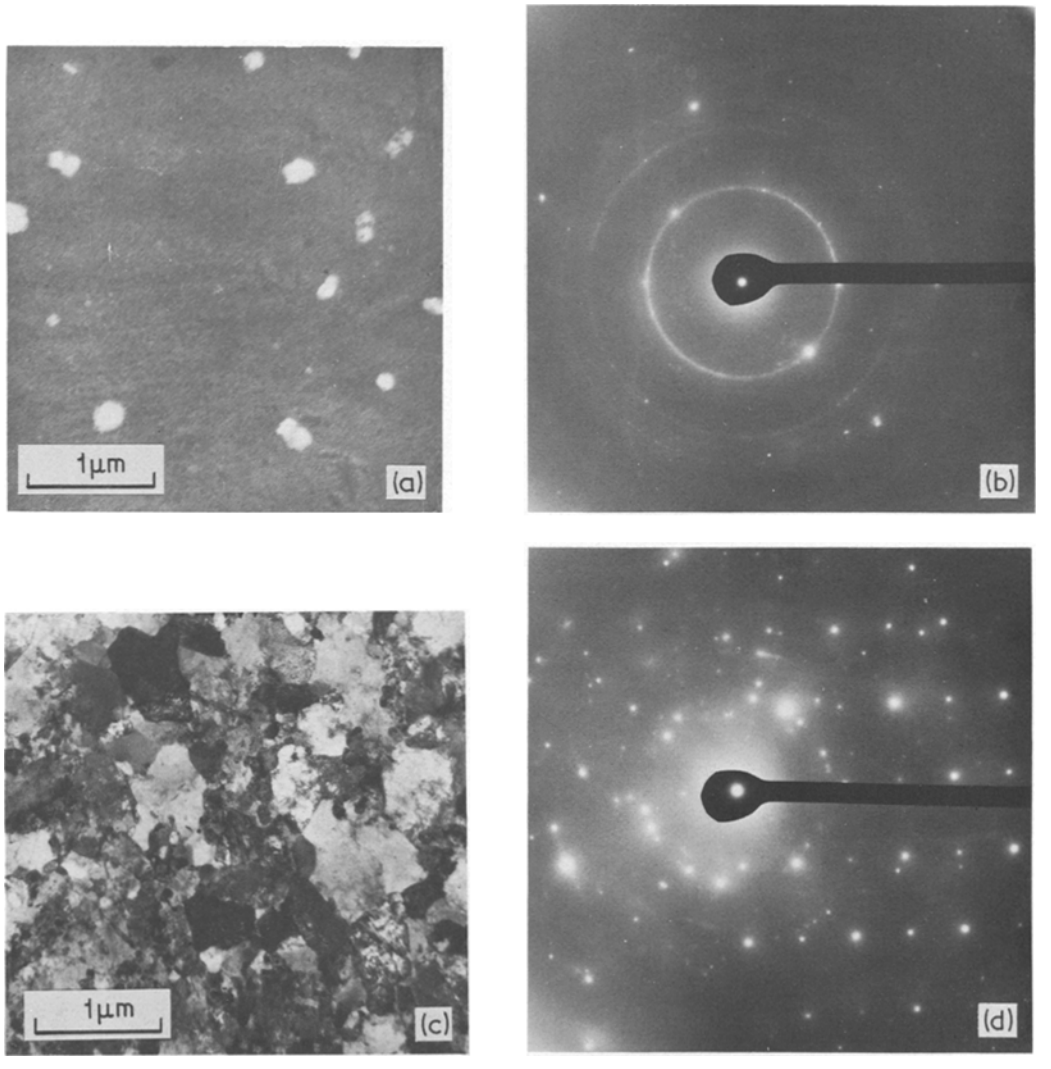

Figure 7 Precipitation of Ni_3Al in Al–78.8 at.% Ni: (a) and (b) after 30 sec at 800° C showing ~ 2000 Å Ni_3Al particles in a matrix which has transformed to supersaturated f c c (Ni); (c) and (d) after 3 min at 800° C showing final equi-axed grain structure, ~ 0.5 μm in size, of Ni_3Al + Ni phase mixture.

identical to NiAl with 33% of the nickel sites vacant, and the vacancies ordered in such a way that every third plane of nickel atoms perpendicular to $\langle 1\,1\,1\rangle_{NiAl}$ is absent [18]. This vacancy ordering gives rise to extra superlattice reflections on X-ray and electron diffraction patterns (see Figs. 5d and 6d).

Over the composition range 29.2 to 72.4 at.% Ni, vapour-quenched Al–Ni alloys transform initially to a single phase with an NiAl structure. Thus, by a combination of vapour-quenching and partial annealing the NiAl phase field can be extended well beyond its equilibrium limits. The formation of NiAl from the vapour-quenched alloys requires only limited short-range diffusion, and must be very favourable energetically given that NiAl is a stable phase with a high melting point [17]. As measured by the precipitation temperature (see Table I), the vapour-quenched alloys are quite resistant to this transformation, presumably as a consequence of their low vacancy concentration (see previous discussion). In vapour-quenched Al–55.2 at.% Ni, formation of NiAl is followed at higher temperatures by precipitation of Ni_3Al by diffusion-controlled growth. In vapour-quenched alloys containing 29.2, 39.5 and 42.5 at.% Ni, the second stage of annealing involves the formation of Ni_2Al_3. For short anneal-

ing times in these alloys, there is sufficient diffusion for atoms to become ordered on an NiAl lattice; longer annealing times are required to allow off-stoichiometry vacancies to become ordered on the nickel sub-lattice and give rise to Ni_2Al_2 superlattice reflections. In Al–29.2 at.% Ni, this latter stage is associated with long-range diffusion and growth of $NiAl_3$ particles.

Precipitation of $NiAl_3$ from vapour-quenched Al–25.0 at.% Ni takes place by slow nucleation and very rapid growth. An essential criterion for such rapid growth is that the transformation involves a change in structure with no change in composition and is therefore not limited by solute diffusion. In each of Al–25.0, 39.5 and 55.2 at.% Ni alloys, the precipitating phase has the same composition as the quenched alloy, and this is very nearly true for Al–78.8 at.% Ni. However, precipitation of Ni_2Al_3, NiAl and Ni_3Al respectively from Al–39.5, 55.2 and 78.8 at.% Ni takes place by copious nucleation and relatively slow growth (see Table II). The growth rate of Ni_3Al is quite high but this is probably a consequence of the high temperature required to initiate the preceding b c c to f c c transformation. The type of precipitation observed in Al–25.0 at.% Ni has been seen previously, but only in crystallisation from an amorphous alloy structure [19, 20]. A secondary requirement for such rapid growth may be that the parent phase is amorphous. The latent heat of an amorphous to crystalline transformation is greater than that of a crystalline to crystalline transformation; thus the reaction may be self-heating with a continually increasing growth rate. This suggests that the anomalous as-quenched structure of alloys with 25.0 to 39.5 at.% Ni is an f c c/amorphous mixture. This structure has been considered previously to be unlikely, although consistent with the observed electron diffraction patterns [1].

The surface of a growing $NiAl_3$ particle is rough on the same scale as the as-quenched grain size (Fig. 3). This is reasonable in view of previous work which suggests that $NiAl_3$/liquid interfaces are faceted [21]. However, because of the small grain size in vapour-quenched alloys, growth of $NiAl_3$ is macroscopically isotropic. The conditions for dendritic growth are an isotropic transformation with a rapid growth rate, which becomes limited by solute diffusion [22]. Thus, in vapour-quenched Al–11.3 and 29.2 at.% Ni, solute diffusion is required for precipitation of $NiAl_3$. In these alloys, $NiAl_3$ particles grow with a perturbed interface, although without a fully-developed dendritic structure.

5. Conclusions

Non-equilibrium phases in vapour-quenched Al–Ni, Al–Cu and Al–Fe alloys show considerable thermal stability because of a low as-quenched vacancy concentration. Highly supersaturated f c c alloys transform to equilibrium with a precipitation sequence:

supersaturated f c c ~ 50 Å grain size	→	grain growth to ~ 200 Å grain size	→	precipitation to equilibrium $NiAl_3$, $CuAl_2$ or $FeAl_3$

The occurrence of grain growth, and the direct precipitation of equilibrium phases without formation of GP zones or intermediate phases, are consequences of the very small grain size of as-quenched alloys. Precipitation of $NiAl_3$ from vapour-quenched Al–25 at.% Ni is by slow nucleation and rapid isotropic growth which suggests that the as-quenched alloy is an f c c/amorphous phase mixture; in non-stoichiometric alloys, $NiAl_3$ particles grow with a perturbed interface. Vapour-quenched alloys containing 29.2 to 72.4 at.% Ni all transform initially to an NiAl-type ordered b c c phase. In some of the alloys, this is followed by vacancy ordering to form Ni_2Al_3 and precipitation of $NiAl_3$ or Ni_3Al.

Acknowledgement

The authors are grateful to the Science Research Council and Alcan International Ltd. for financial support of this research programme.

References

1. B. CANTOR and R. W. CAHN, *Acta Met.*, in press.
2. L. HOLLAND and C. R. D. PRIESTLAND, *Vacuum* **22** (1972) 133.
3. R. E. L. COX and L. HOLLAND, *Nature Phys. Sci.* **241** (1973) 149.
4. A. TONEJC and A. BONEFACIĆ, *Fizika* **2** (1970) 81.
5. A. TONEJC, D. ROCAK and A. BONEFACIĆ, *Acta Met.* **19** (1971) 311.
6. M. G. SCOTT and J. A. LEAKE, *ibid* **23** (1975) 503.
7. M. G. SCOTT, Ph.D. thesis, Cambridge (1973).
8. M. M. JACOBS, A. G. DOGGETT and M. J. STOWELL, *Fizika* **2** (Suppl.) (1970) 18.
9. M. M. JACOBS, A. G. DOGGETT and M. J. STOWELL, *J. Mater. Sci.* **9** (1974) 1631.

10. S. C. ARGAWAL and H. HERMAN, in "Phase Transitions 1973", (Pergamon Press, Oxford 1973) p. 207.
11. A. KELLY and R. B. NICHOLSON, *Prog. Mat. Sci.* **10** (1963) 151.
12. K. G. LATIMER, P. J. READ and T. D. W. REYNOLDS, presented at conference on "Modern Metallography", Oxford (1973).
13. K. D. KRISHNANAND and R. W. CAHN, "Proceedings of the 2nd International Conference on Rapidly Quenched Metals", Boston 1975, in press.
14. G. THURSFIELD and M. J. STOWELL, *J. Mater. Sci.* **9** (1974) 1644.
15. G. THOMAS and R. H. WILLENS, *Acta Met.* **12** (1964) 191; **13** (1965) 139; **14** (1966) 1385.
16. J. A. MCCOMB, S. NENNO and M. MESHII, *J. Phys. Soc. Japan* **19** (1964) 1691.
17. M. HANSEN and K. ANDERKO, "Constitution of Binary Alloys" (McGraw-Hill, New York, 1958).
18. A. TAYLOR and N. J. DOYLE, *J. App. Crys.* **5** (1972) 201, 210.
19. J. M. LUCAS, D. Phil. thesis, Sussex (1969).
20. U. KÖSTER and P. WEISS, *J. Non-Cryst. Solids* **17** (1975) 359.
21. D. JAFFREY and G. A. CHADWICK, *Met. Trans.* **1** (1970) 3389.
22. R. D. DOHERTY in "Crystal Growth", vol. 1 edited by B. R. Pamplin (Pergamon Press, Oxford, 1974).

Received 28 October and accepted 17 November 1975.